

PCCP

Accepted Manuscript



This is an *Accepted Manuscript*, which has been through the Royal Society of Chemistry peer review process and has been accepted for publication.

Accepted Manuscripts are published online shortly after acceptance, before technical editing, formatting and proof reading. Using this free service, authors can make their results available to the community, in citable form, before we publish the edited article. We will replace this *Accepted Manuscript* with the edited and formatted *Advance Article* as soon as it is available.

You can find more information about *Accepted Manuscripts* in the [Information for Authors](#).

Please note that technical editing may introduce minor changes to the text and/or graphics, which may alter content. The journal's standard [Terms & Conditions](#) and the [Ethical guidelines](#) still apply. In no event shall the Royal Society of Chemistry be held responsible for any errors or omissions in this *Accepted Manuscript* or any consequences arising from the use of any information it contains.

Page 1 of 8 Physical Chemistry Chemical Physics

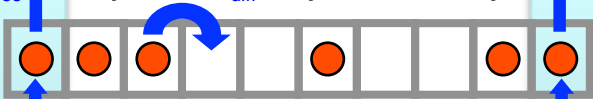
W_{des}

W_{diff}

W_{des}

W_{ads}

W_{ads}



Equilibration Processes during Gas Uptake Inside Narrow Pores

Cite this: DOI: 10.1039/x0xx00000x

Joshua M. Vann, Samantha L. Molnar, and M. Mercedes Calbi^a

Received 00th January 2012,
Accepted 00th January 2012

DOI: 10.1039/x0xx00000x

www.rsc.org/

We analyze the adsorption kinetics of a gas in contact with the open ends of a narrow longitudinal pore, where gas transport along its interior occurs via single-file diffusion mechanisms. By implementing a Kinetic Monte Carlo simulation of the gas dynamics, we obtain the overall change in gas uptake inside the pore and the concentration profile of the adsorbed phase as the system evolves towards equilibrium. Typically, higher external pressure leads to faster kinetics as it happens for adsorption on open surfaces. However, when the pore is exposed to gas at very high pressures, blockage events near the ends of longer pores can slow down the overall adsorption, with desorption and internal diffusion eventually becoming the rate limiting processes. We determine the dependence of these phenomena on the amount of gas adsorbed, binding energy and length of the pore.

Introduction

Gas adsorption in porous materials presents several distinguishing features when compared to uptake on open surfaces.¹⁻⁷ The intrinsic confinement imposed by the particular morphology of the pores determines equilibrium properties of the adsorbed phase such as the isosteric heat of adsorption and overall uptake. In addition, the accessibility to the pore's internal space may be limited by the characteristics of the openings and the processes that occur near the ends of the pore. These are the factors that mostly control the kinetics of adsorption as the adsorbed phase comes to equilibrium with the external gas, affecting the speed of the process and the evolution of the concentration profiles inside the pore. This work is mainly focused on those kinetic processes that occur during gas uptake inside simple, relatively narrow pores.

Experimental reports of gas uptake inside porous nanostructures tend to exhibit a significant wider dispersion when compared to similar measurements done on non-porous adsorbents. In particular, discrepancies observed in gas uptake of open-ended carbon nanotubes provided us with the initial motivation to explore possible kinetic effects that could lead to unusually slow adsorption rates and therefore impact the experimental determination of the equilibrium uptake.^{8,10} On the other hand, the use of many porous nanostructures such as carbon nanotubes, zeolites, or metal-organic frameworks for storage and separation applications depends heavily on our basic understanding of not only equilibrium properties but also on how different gases are able to access those internal pores

and what are the factors that influence the speed of such processes.¹¹

In a previous work, we analyzed the adsorption kinetics of gases in different regions of a nanotube bundle by implementing a Kinetic Monte Carlo simulation on a linear lattice of sites.¹² We distinguished two broadly defined kinds of phases as: a) external, when gas is adsorbed on exterior of the bundle including grooves between the tubes and tubes' external surface, and b) internal, when gas populates the interior of the tubes or the interstitial spaces between them. In both cases, we found that the equilibration time decreases with the final equilibrium coverage of the lattice, which is mainly due to faster occupation rates generated by the increasing external pressure. If the interaction between the adsorbate molecules is relatively weak compared to the adsorbate-surface interaction, the trend tends to be linear with a slope that increases with the binding energy.¹² Recent experimental results particularly confirmed this observation for simple gases adsorbing on carbon nanotube bundles thus providing validity to our model and methods.¹³ We observed, however, two main differences between the trends of the external and internal phases: 1) equilibration times for the internal phases were orders of magnitude longer, as we could expect since access to the internal lattice sites would only happen through diffusion from the end sites, and 2) while the equilibration time approaches zero when the lattice of an external phase becomes fully occupied, that is not the case for the internal phases. We found that equilibration times typically remain finite at monolayer coverage, with larger values corresponding to weaker binding

energies.¹² In order to explain this behaviour, we investigate here the elementary processes involved in the adsorption kinetics of these internal phases, and analyze the competing effects of internal diffusion and external pressure that lead the system to equilibrium. We first examine how the coverage profile inside the pore evolves with time and explore its dependence on the binding energy, final uptake and the length of the pore. We then focus on the high coverage regime where we observe that the equilibration speed ceases to be determined by the external pressure and it rather depends on the ability of the molecules to move inside the pore.

Models and Methods

The computational approach we use in this work is based on the simulation of the gas dynamics during uptake by following a Kinetic Monte Carlo (KMC) algorithm^{12,14} as explained below. We model the pore as a one-dimensional array of L sites, each one providing the same binding energy ϵ . The pore is exposed to a gas of particles characterized by a temperature T and chemical potential μ . Direct adsorption/desorption from the gas only occurs at the end sites while the internal sites become occupied as the molecules move along the lattice. We calculate the total energy of a particle adsorbed on site i as:

$$E_i = \epsilon + \sum_{j, NN} \epsilon_{int} n_i n_j \quad (1)$$

where ϵ_{int} represents the gas-gas interaction between a pair of nearest-neighbour (NN) particles.

We simulate the adsorption dynamics in the pore by letting the system evolve from an initially empty lattice until the final coverage corresponding to equilibrium with the gas at given values of T and μ is reached. This equilibration occurs by means of elemental processes of adsorption/desorption from the gas and diffusion along the lattice. Within the KMC scheme, this is achieved by performing the following steps:

1. At any given time, we calculate transition probabilities W for adsorption/desorption (only at the end sites) as

$$\frac{W_{ads}}{W_{des}} = \exp[-\beta(E_i - \mu)] \quad (2)$$

and diffusion across internal sites as

$$\frac{W_{i \rightarrow j}}{W_{j \rightarrow i}} = \exp[-\beta(E_j - E_i)] \quad (3)$$

In these equations, $\beta=1/(k_B T)$ with k_B being the Boltzmann constant.

2. Based on these probabilities, a selection rule (as prescribed by the KMC algorithm¹⁴) is used to choose the transition that takes place and evolves the system from one state to another.

3. The time is then accordingly advanced, and the new coverage (and any other quantity desired at that time) is calculated.

These steps are repeated until the coverage stops changing with time, i.e. equilibrium with the gas phase has been reached. In this way, we find the overall uptake inside the pore as a function of time as well as the concentration profiles along the pore at the respective times.

In the following section, we first analyze these results to determine the dependence of the concentration profiles with the external pressure (or final coverage), the length of the pore and the binding energy. The shape of these curves reveals the way particles from the gas access the interior of the pore as the uptake progresses, and how adsorption/desorption rates compete with diffusion rates at different times until equilibrium is reached. In the second part of the Results section, we focus on the processes that happen at relatively high coverage: It typically takes less time for lower binding systems to reach a given coverage,¹² however, we sometimes observe a crossover between these trends as the coverage increases. We compare the concentration profiles and directly count events to provide an explanation for this behaviour.

Results

In order to fully describe the adsorption dynamics of a gas in an open-ended pore, we examine how the overall uptake and the concentration profiles change with time, for different values of the external pressure, length of the pore and binding energy of the sites. In all cases, we are considering a system for which the relative size of the adsorbate to the pore width allows the formation of a single line of adsorbed molecules (single-channel uptake; see for example Ref. 12 and 15). In order to simplify the analysis, the results presented in the first two sections do not include molecule-molecule interactions; we show additional results in section III that illustrate the effects of these interactions on the previously described dynamics.

I. Equilibration Curves and Concentration Profiles

In Figure 1 we show the time evolution of the coverage and the corresponding concentration profiles as the system advances towards equilibrium. From top to bottom, each pair of graphs in a row correspond to increasing values of the external gas pressure which leads to increasing final coverages at equilibrium. Since the equilibration times will be different in each case, we compare the profiles at the same relative times with respect to equilibrium, i.e. when the systems are at equivalent stages of the equilibration process. We observe that at higher loading, the end sites reach the final coverage far faster than the middle sites. When fewer particles are absorbed inside a pore, they tend to be more evenly distributed. This basically happens because increased external pressure generates adsorption rates at the ends that are much higher than diffusion rates inside the pore; therefore, as soon as the end site becomes vacant, adsorption events at the end sites happen much more frequently than diffusion across internal sites. This is more prominent for longer pores as shown in Figure 2.

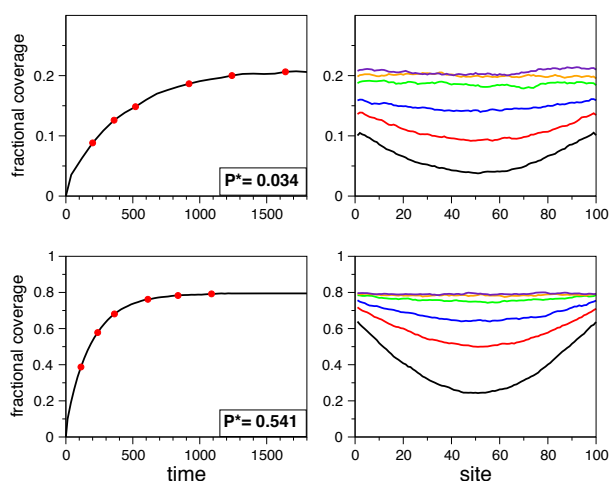


Figure 1. Overall uptake as a function of time (left) and corresponding concentration profiles (right) at the times indicated by the red dots in the equilibration curves. Ends enjoy a greater coverage earlier in the evolution until the profile becomes a uniform distribution at equilibrium. Upper panels show the evolution towards 20% lattice occupation while 80% final occupation is illustrated in the bottom row. Corresponding values of the reduced pressure $P^* = \exp(\beta\mu)$ are also indicated ($L=100$ sites and $\beta\epsilon=-2$).

In Figure 2 we compare the profiles in pores of different length for increasing pressures. At higher loading, the end sites of longer tubes adsorb particles much faster than the middle sites, reaching the final equilibrium coverage almost instantly; when the external pressure decreases, particle diffusion occurs at a relatively much faster rate, leaving the ends at lower occupancy. The ends of longer tubes are able to maintain better equilibrium with gas due to the increased number of diffusion processes that are needed to occupy the internal sites of the tube.

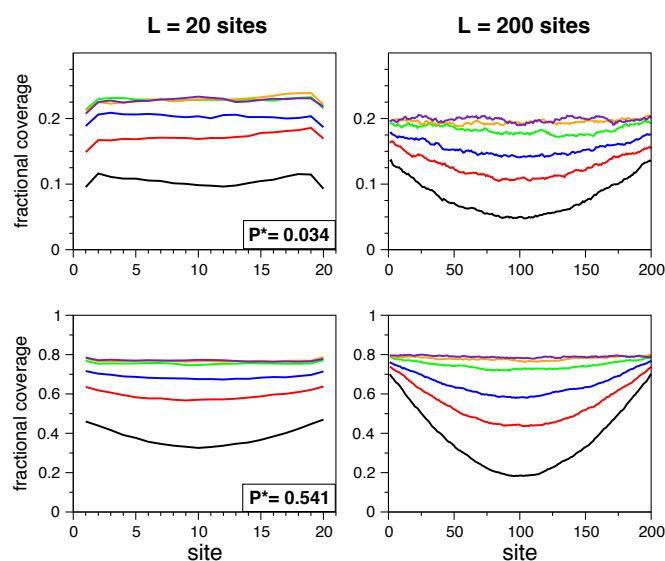


Figure 2. Concentration profiles reaching increasing loading for pores with same binding but of different length. Profiles taken at the same relative time with respect to final equilibration time: 0.1, 0.2, 0.3, 0.5, 0.7, and 0.9; $P^* = \exp(\beta\mu)$ and $\beta\epsilon=-2$.

We illustrate the effect of the binding strength on the profiles in Figure 3. In this case, regardless of the final loading, stronger binding leads to mostly uniform adsorption within the pore. The end sites and the middle sites are occupied at the same rate, at all times during the evolution. Increased binding produces much lower adsorption rates at the ends, leaving enough time for the particles to fully diffuse inside the tube.

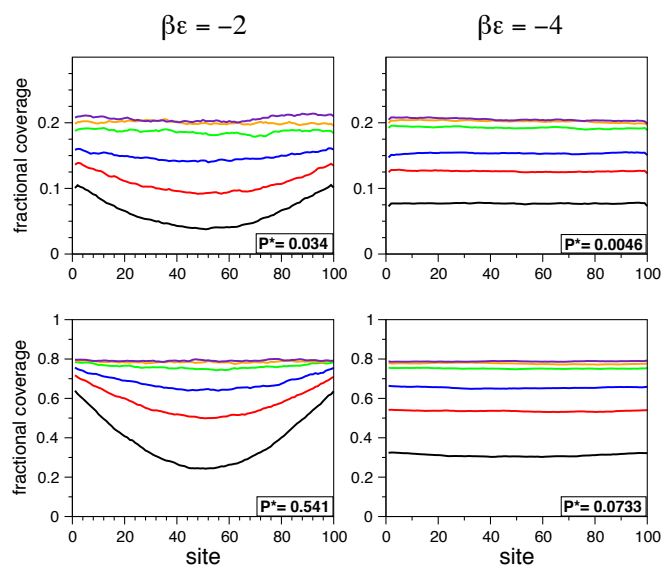


Figure 3. Concentration profiles reaching increasing loading for pores with same length ($L=100$ sites) but of different binding. Pores with stronger binding require lower P^* values to reach the same final coverage. Profiles are taken at the same relative time with respect to the final equilibration time as in Fig. 2.

II. High Coverage Dynamics: Blockage Effects

We now turn our attention to the overall kinetic behaviour as described by the equilibration time as a function of the final coverage. From the curves that show the overall uptake evolution with time, we determine the time it takes for the system to equilibrate and reach its final coverage. We plot this equilibration time as a function of the final coverage in Figure 4, for different values of the binding energy and length of the pore.

In all cases we observe a decreasing trend, with higher slopes corresponding to higher binding. This is similar to what we have observed previously for the open surface kinetics,¹² and can be attributed directly to the dominant effect of the external pressure on the adsorption rates: Higher pressure is needed to reach higher final uptake (for the same binding strength); conversely, to reach the same final coverage, higher pressure is needed for a particle to bind to a weaker binding site. In both cases, higher pressure means faster adsorption rates. However, if we compare two curves corresponding to different binding, we observe a crossover at high coverage where these trends are reversed, making equilibration times longer for the weaker binding pore. We also notice that the

crossover coverage tends to get higher as the length of the pore shortens to the point that no crossover is observed at all if the pore is very short ($L=20$ sites).

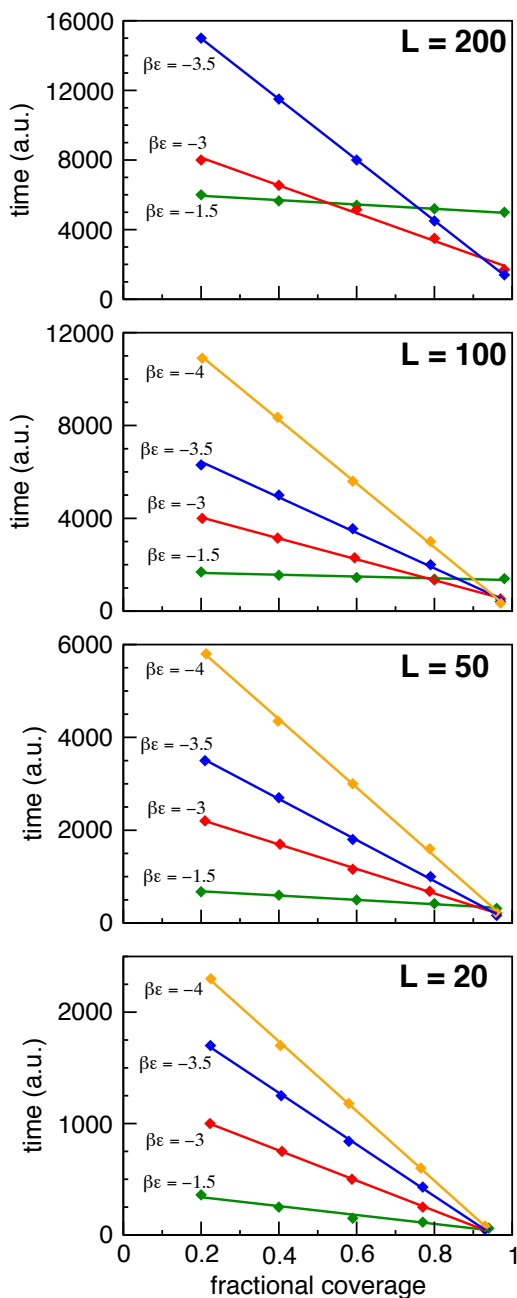


Figure 4. Equilibration time as function of final loading for pores of decreasing length. The lines in each panel show the trends corresponding to different binding ($\beta\epsilon$) for a pore of a given length.

In order to understand why this happens, we compare in Figure 5 the concentration profiles *at the same time*, for coverage values before and after the crossover. To highlight the relative speed of equilibration of one system with respect to the other, lines shown with the same color in the different panels

correspond to profiles at the same absolute time. For the case shown in the figure ($L=100$ sites), the crossover between the strong ($\beta\epsilon = -4$) and weak ($\beta\epsilon = -2$) binding trends occurs after approximately 90% of lattice occupation. Before the crossover (at about 80% occupation), we observe a clear advantage of the weaker binding system. This is mainly due to a faster adsorption rate at the end sites. After the crossover, the pressure is so high that the end sites are practically at equilibrium with the gas at all times. However, diffusion events are drastically reduced due to the higher occupancy of the sites closer to the ends (10% of the lattice sites right next to the ends have more than 0.5 coverage at the earliest time). Therefore, while the higher pressure provides some advantage near the ends, the occupancy of the middle sites remains relatively low and the overall equilibration process is then delayed.

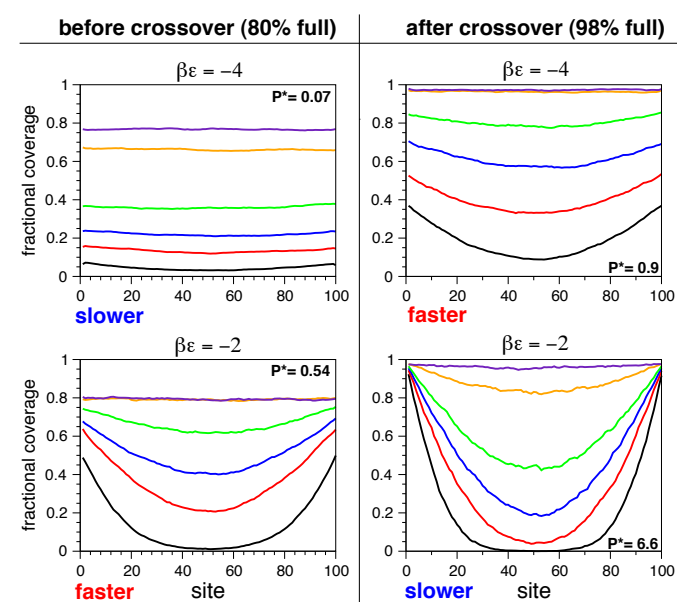


Figure 5. Concentration profiles before (left panels, final coverage 0.8) and after (right panels, final coverage 0.98) the crossover. When comparing top to bottom panels, profiles taken at the same time are shown with the same color. While the increased pressure provides a clear advantage to the weak binding pore at lower occupation, the situation is reversed if the final coverage is closer to full occupation.

We analyze the relative importance of the adsorption to the diffusion events and how that impacts the overall speed of the process by looking specifically at the events that are happening at the end sites, in order to identify the ones that occur more frequently as the system equilibrates. In Figure 6, we compare both systems before the crossover: in the faster equilibrating system (weaker binding), adsorption events are much more frequent while the chances to move to the interior are still high. Thus, the overall equilibration time is essentially determined by the external pressure that is needed to achieve adsorption at that specific binding strength.

On the other hand, after the crossover (Figure 7), the system that enjoys a higher adsorption rate ends at a disadvantage

because the higher pressure causes the neighbouring sites to be almost immediately occupied, making the diffusion towards the interior of the pore more difficult and increasing the number of desorption events instead.

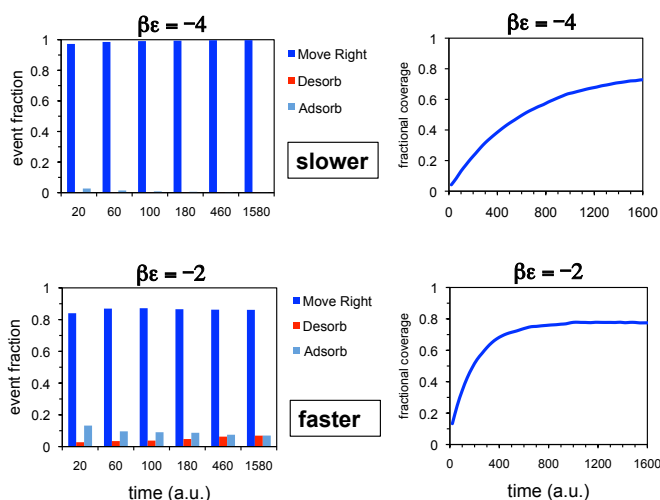


Figure 6. Before the crossover: Left panels show the number events of each kind (percentage of the total) as a function of time; corresponding equilibration curves presented in the right panels demonstrate the advantage of the weaker binding pore. Snapshot times are the same as the ones corresponding to same color lines in Fig. 5.

This blockage effect near the ends of the pore slows down the overall equilibration process; in this case, the lower pressure needed to adsorb particles with stronger binding results in adsorption rates that are more comparable to the diffusion rates, the distribution of particles is more uniform and the system equilibrates faster.

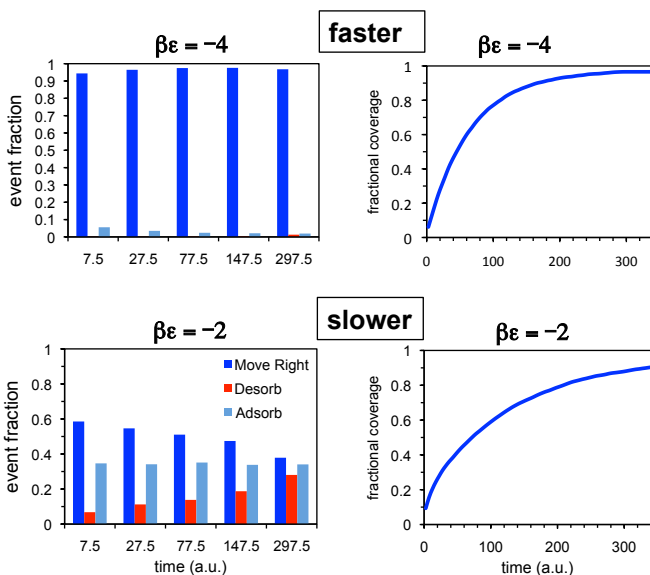


Figure 7. After the crossover: the high pressure at the ends of the weaker binding pore generates a blockage effect that slows down the uptake relative to the stronger binding pore.

Therefore, at very high coverage, the overall adsorption speed is determined by the ability of the particles to move in inside the pore. In that case, it is the system with the lower desorption rate that equilibrates faster. Indeed, this explains our original observation about the equilibration time near monolayer completion following the exponential decay dependence with the binding energy ($W_{\text{des}} \sim \exp(-\beta|\epsilon|)$).¹²

III. Molecular Interaction Effects

In general, within the model described by Eq. 1, attractive interactions between adsorbates generate an increased effective binding to the surface that depends on the coverage.¹² Figure 8 illustrates this effect as we show the overall equilibration time as a function of the coverage for increasingly stronger interactions. Similarly to what we observed previously for open surfaces,¹² equilibration times become longer as the interactions increase (as a result of the increased effective binding). In addition, the coverage dependence shows a maximum that gets closer to full occupancy as the interaction strength increases.

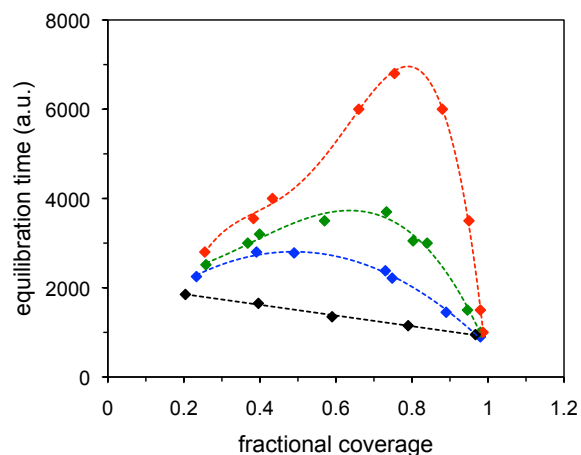


Figure 8. Effect of molecular interactions on the equilibration times ($L=100$, $\beta\epsilon = -2$). The black, straight line corresponds to the non-interacting case. From bottom to top, the curves are for $\epsilon_{\text{int}} = 0.5\epsilon$, ϵ and 2ϵ . Dotted lines are just to guide the eye.

We also explored the effect of the interactions on the concentration profiles. In Figure 9, we show typical curves as the system evolves towards equilibrium. The shape of these curves does not present a significant qualitative change when compared with the non-interacting case.

Finally, we looked at the presence of blockage effects as described in section II. Figure 10 shows the equilibration time for two different binding energies; although the coverage dependence is different when interactions are present, the crossover behaviour still persists.

Conclusions

We have explored the adsorption dynamics of a simple gas entering a narrow pore as a function of the binding energy and

length of the pore. In particular, we focus on understanding the dependence of the overall equilibration time on the binding energy, always in the case where only a single line of atoms can occupy the interior of the pore. If the pore is long enough (which we expect is the case for most practical systems), we find that although higher pressures would lead to faster uptake favouring weaker binding systems, blockage events near the ends of the pore can significantly slow down the adsorption. We have shown that this is the case by examining the concentration profiles as well as directly comparing the frequency of adsorption/desorption events with respect to the diffusion events.

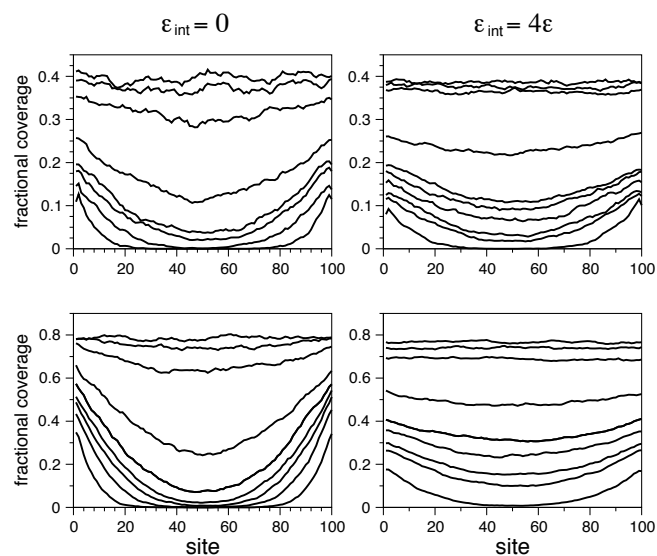


Figure 9. Molecular interactions effects on the concentration profiles ($\beta\epsilon = -2$). The top panels compare the profiles that lead to 40 % final loading and the bottom ones are for 80 % final coverage.

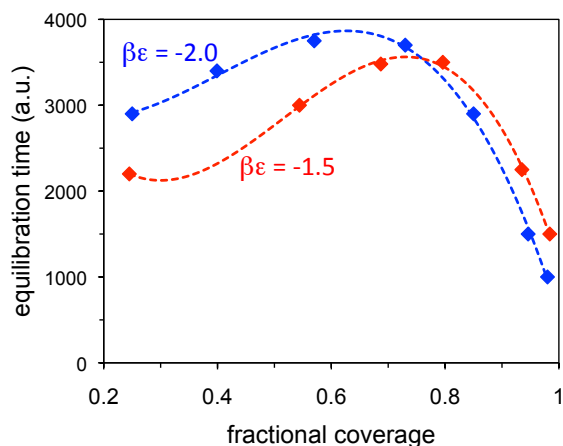


Figure 10. Equilibration time for two different binding energies ($L=100$, $\epsilon_{\text{int}} = \epsilon$). Faster become slower for fractional coverages above 0.75.

Looking at the concentration profiles near the ends, we notice that while higher values of dn/dx (near $t=0$) usually mean shorter equilibration times, there seems to be a threshold value over which a gas build-up develops, slowing down the overall

uptake. This is directly related also to the length dependence since shorter pores do not provide enough space for this to happen. In general, we expect these blockage effects to be present for relatively longer pores and weaker binding energies. However, when comparing dynamics of two different gases (for example for separation purposes), it is important to keep in mind that these effects do depend on the gas pressure (or final coverage), as shown in Figure 4.

We performed several simulations to explore the molecular interactions effects on the dynamics, increasing ϵ_{int} up to 2ϵ (for most simple gases on carbon surfaces for example, gas-gas interactions are not greater than 10-20% of the binding energy). Equilibration times increase significantly due to increased effective binding, as we observed previously.¹² However, we did not find any signs of clustering even at the earliest times in the evolution. This is probably due to the presence of a one-dimensional phase inside the pore; it is likely this changes when considering higher dimensional phases inside wider pores.

Even though a direct, quantitative comparison with available experimental data is not possible at this time, we highlight next some trends seen in experimental studies of adsorption kinetics of gases in different nanoporous materials that can be understood based on our simulation results. For example, a study of Ar adsorption on chemically opened carbon nanotubes found a non-monotonic dependence of the equilibration time with coverage similar to the ones shown in Figure 8.¹⁰ Likewise, it was observed that equilibration times of O_2 adsorbing on the metal-organic framework ZIF-8 decrease rapidly with coverage as the channels get fully filled.¹⁶ In another experimental study of CF_4 and Ar on another class of metal-organic frameworks, the authors observed a much more rapid equilibration of Ar as compared to CF_4 which could be expected based on the relatively weaker binding of Ar (as observed in Figure 4).¹⁷ Finally, measurements of Ne and CO_2 adsorption on aggregates of chemically opened carbon nanohorns show a decreasing trend of the equilibration time with coverage for Ne while the opposite is observed for CO_2 in similar coverage intervals. This is very likely due to the much more dominant effect of the molecular interactions in the case of carbon dioxide as compared to Ne (as seen in Figure 8).¹⁸

Rather than focusing on a particular gas or adsorbent, in this paper we looked for general trends in the gas dynamics that would help to understand the kinetic behaviour of seemingly diverse systems. Therefore, we focus on the elementary processes that could help explain the adsorption kinetics in porous adsorbents such as open-end carbon nanotubes, zeolites or metal-organic frameworks. Each system is characterized by different parameters and we provide here basic elements to understand how different observed trends can depend on those parameters, as a first step in guiding the design of systems for specific applications or the inclusion of other particular effects for modelling more complicated phenomena.

Acknowledgements

We acknowledge the support provided by the National Science Foundation through Grants CBET-1064384 and DMR-1006428.

Notes and references

^a Department of Physics and Astronomy, University of Denver, Denver, Colorado 80208, USA.

- 1 L. J. Dunne, G. Manos (Eds.), Adsorption and Phase Behaviour in Nanochannels and Nanotubes (Springer, London, 2010).
- 2 J. Karger, D. M. Ruthven, D. N. Theodorou, Diffusion in Nanoporous Materials (Wiley-VCH, Weinheim, 2012).
- 3 D. D. Do, Adsorption Analysis: Equilibria and Kinetics (Imperial College Press, London, 1998).
- 4 Rolando M. A. Roque-Malherbe, Adsorption and Diffusion in Nanoporous Materials (Taylor & Francis Group, 2007).
- 5 L. D. Gelb, K. E. Gubbins, R. Radhakrishnan and M. Sliwinski-Bartkowiak, *Rep. Prog. Phys.*, 1999, **62**, 1573.
- 6 P. A. Monson, *J. Chem. Phys.*, 2008, **128**, 084701.
- 7 S. K. Bhatia, M. Rincon Bonilla and D. Nicholson, *Phys. Chem. Chem. Phys.*, 2011, **13**, 15350.
- 8 A. D. Migone and S. Talapatra, Encyclopedia of Nanoscience and Nanotechnology (Nalwa, H. S., Ed., American Scientific Publishers, Los Angeles, 2004) p. 749-767.
- 9 M. M. Calbi, J. L. Riccardo, *Phys. Rev. Lett.*, 2005, **94**, 246103.
- 10 D. S. Rawat, M. M. Calbi, A. D. Migone, *J. Phys. Chem. C*, 2007, **111**, 12980.
- 11 R. T. Yang, Adsorbents: Fundamentals and Applications (John Wiley & Sons, Inc, Hoboken, 2003).
- 12 J. T. Burde and M. M. Calbi, *J. Phys. Chem. C*, 2007, **111**, 5057.
- 13 D. S. Rawat, V. Krungleviciute, L. Heroux, M. Bulut, M. M. Calbi, A. D. Migone, *Langmuir*, 2008, **24**, 13465.
- 14 F. M. Bulnes, V. D. Pereyra, J. L. Riccardo, *Phys. Rev. E*, 1998, **58**, 86.
- 15 R. A. Trasca, M. M. Calbi, M. W. Cole, *Phys. Rev. E*, 2002, **65**, 061607.
- 16 B. Russell, J. Villaroel, K. Sapag, A. D. Migone, *J. Phys. Chem. C*, 2014, **118**, 28603.
- 17 V. Krungleviciute, K. Lask, A. D. Migone, J.-Y. Lee, J. Li, *AIChE J.*, 2008, **54**, 918.
- 18 V. Krungleviciute, C. A. Ziegler, S. R. Banjara, M. Yudasaka, S. Iijima, A. D. Migone, *Langmuir*, 2013, **29**, 9388.